

# PCCP

Accepted Manuscript



This is an *Accepted Manuscript*, which has been through the Royal Society of Chemistry peer review process and has been accepted for publication.

*Accepted Manuscripts* are published online shortly after acceptance, before technical editing, formatting and proof reading. Using this free service, authors can make their results available to the community, in citable form, before we publish the edited article. We will replace this *Accepted Manuscript* with the edited and formatted *Advance Article* as soon as it is available.

You can find more information about *Accepted Manuscripts* in the [Information for Authors](#).

Please note that technical editing may introduce minor changes to the text and/or graphics, which may alter content. The journal's standard [Terms & Conditions](#) and the [Ethical guidelines](#) still apply. In no event shall the Royal Society of Chemistry be held responsible for any errors or omissions in this *Accepted Manuscript* or any consequences arising from the use of any information it contains.



Journal Name

ARTICLE

## Phospholamban spontaneously reconstitutes into Giant Unilamellar Vesicles where it generates a cation selective channel

S. Smeazzetto,<sup>a</sup> F. Tadini-Buoninsegni,<sup>a</sup> G. Thiel,<sup>b</sup> D. Berti\*<sup>c</sup> and C. Montis<sup>c</sup>Received 00th January 20xx,  
Accepted 00th January 20xx

DOI: 10.1039/x0xx00000x

www.rsc.org/

Phospholamban (PLN) is a small integral membrane protein, which modulates the activity of the Sarcoplasmic Reticulum  $\text{Ca}^{2+}$ -ATPase (SERCA) of cardiac myocytes. PLN, as a monomer, can directly interact and tune SERCA activity, but the physiological function of the pentameric form is not yet fully understood and still debated. In this work, we reconstituted PLN in Giant Unilamellar Vesicles (GUVs), a simple and reliable experimental model system to monitor the activity of proteins in membranes. By Laser Scanning Confocal Microscopy (LSCM) and Fluorescence Correlation Spectroscopy (FCS) we verified a spontaneous reconstitution of PLN into the phospholipid bilayer. In parallel experiments, we measured with the patch clamp technique canonical ion channel fluctuations, which highlight a preference for  $\text{Cs}^+$  over  $\text{K}^+$  and do not conduct  $\text{Ca}^{2+}$ . The results prove that PLN forms, presumably in its pentameric form, a cation selective ion channel.

### Introduction

Contraction and relaxation of cardiac myocytes is associated with a periodic modulation in the concentration of  $\text{Ca}^{2+}$  in the cytosol.<sup>1,2</sup> A significant contribution to this dynamic process is provided by the  $\text{Ca}^{2+}$ -ATPase (SERCA), which is present in the sarcoplasmic reticulum (SR). It maintains a low cytosolic calcium concentration by pumping excess cytosolic  $\text{Ca}^{2+}$  into the SR.<sup>3,4</sup> The activity of SERCA is modulated by Phospholamban (PLN), a small integral membrane protein in the SR of cardiomyocytes. The functional role of the 6kDa PLN protein, which is built of only 52 amino acids, is of great biomedical relevance. In recent years several mutants were discovered in human PLN, which are causally related with dilated cardiomyopathy.<sup>1</sup> Because of the key significance in fine-tuning of SERCA activity, the PLN protein is now considered as a highly potential pharmacological target for treating cardiovascular disorders.<sup>5</sup>

Concerning function, it is well established that PLN monomers interact with SERCA and as a consequence inhibit the activity of the  $\text{Ca}^{2+}$ -ATPase. PLN can be phosphorylated, which terminates the PLN/SERCA interaction and SERCA inhibition; the result is a stimulation of  $\text{Ca}^{2+}$  pumping into the SR lumen. The PLN protein is not only present in the monomeric form but also as a pentamer.<sup>1</sup> The two oligomeric states seem to be the

result of a simple equilibrium since they are present not only in native membranes but also in micelles formed by the detergent sodium dodecyl sulfate and after reconstitution in phospholipid bilayers.<sup>6</sup> The formation of PLN pentamers is well supported by Fluorescence Resonance Energy Transfer (FRET) experiments, which confirm that PLN can generate pentamers in lipid vesicles<sup>7</sup>, in lipid bilayers<sup>8</sup>, in Sf21 insect cells<sup>9</sup> and in cultured AAV-293 cells.<sup>10</sup>

While it is well established that the PLN monomer interacts directly with SERCA and modulates the activity of the  $\text{Ca}^{2+}$  pump, the physiological function of the pentameric form is not yet fully understood. The current debate is on whether the pentameric form of PLN serves only as an intermediate storage for active monomers<sup>11</sup> or whether the PLN pentamer can generate ion channel activity.<sup>12,13</sup> In order to address this issue, further insight into the functionality of the pentameric PLN is needed. However, the study of ion channels and transporters in membranes of intracellular organelles is still challenging. The main reason is that organelles are too small and difficult to access with micro-electrodes inside living cell. Thus, direct evidence for the activity of PLN inside cells is not yet available. This experimental hurdle can be overcome by reconstituting purified membrane proteins in experimental models of biological membranes (biomimetic membranes). This allows studying phenomena and processes that are not easily addressed *in vivo* or even in cells. Functional studies on PLN, which were performed in biomimetic membranes such as Bilayer Lipid Membranes (BLMs) and Tethered Lipid Membranes (tBLMs), suggested that PLN can indeed generate canonical ion channel fluctuations, which can be modulated by a specific PLN antibody (Ab PLN).<sup>12-16</sup> Moreover, comparative electrophysiological studies of non-phosphorylated versus phosphorylated PLN and experiments with PLN mutants, have shown that structural modifications of the PLN protein can

<sup>a</sup> Department of Chemistry "Ugo Schiff", University of Florence, Firenze, Italy

<sup>b</sup> Plant Membrane Biophysics, TU-Darmstadt, Darmstadt, Germany

<sup>c</sup> Department of Chemistry "Ugo Schiff" and CSGI, University of Florence, Firenze, Italy

\* Debora Berti Department of Chemistry "Ugo Schiff", University of Florence, via della Lastruccia 3, 50019 Sesto Fiorentino, Italy. email: debora.berti@unifi.it; phone: +39 055 457 3038

Electronic Supplementary Information (ESI) available: additional Fluorescence Correlation Spectroscopy data. See DOI: 10.1039/x0xx00000x

affect the electrical activity of the channels.<sup>12</sup> These results suggested that PLN is not only affecting SERCA via a direct interaction but presumably also via its channel function. The modulation of PLN channel activity by phosphorylation or by mutants presumably alters the transport properties of the SR. This in turn may regulate SERCA activity by a modulation of charge balancing during  $\text{Ca}^{2+}$  uptake<sup>12</sup>.

Previous studies have suggested that the pentameric form of PLN is responsible for the channel activity.<sup>12,15</sup> A polymer exclusion method, which allows estimation of the pore size of a channel<sup>17–19</sup> has been applied to PLN reconstituted in BLMs. The results of these experiments support the view that the central pore, which is formed by the PLN pentamer, can serve as channel pore.<sup>12</sup> It is frequently argued that BLMs measurements bear the risk of artifacts and that residual organic solvent, which is used in the preparation procedure, or the poor intrinsic stability of bilayers, could cause channel-like activity independent on any protein. Also data from tBLMs recordings are frequently criticized for possible experimental artifacts. In this case the criticism arises from the small ionic reservoir at one side of the phospholipid bilayer, as well as from the solid support, which could alter the bilayer fluidity. Because of these critical concerns on experimental aspects the experimental evidence for an ion-channel function of PLN is not universally accepted.<sup>11</sup> An alternative system to tBLMs and BLMs for measuring PLN activity is Giant Unilamellar Vesicles (GUVs). These micron-sized spherical shells are composed of a free-standing and solvent-free bilayer. They have a high stability and a curved surface. Among biomimetic membranes, GUVs are recognized as a very suitable and reliable biomimetic membrane,<sup>20–22</sup> and they are useful to investigate the function of peptides<sup>23</sup>, ion channels<sup>24,25</sup> and transporters<sup>26</sup>. Moreover, due to the free-standing properties and the presence of solution on both sides of the membrane, GUVs also allow to study reconstituted membrane proteins both by optical and electrophysiological techniques.

In this work we characterize the reconstitution of PLN into GUVs and investigate the channel function in this simple but reliable biomimetic model. By conjugating the PLN protein with a fluorescent tag, it was possible to study PLN both at a microscopic level by Laser Scanning Confocal Microscopy (LSCM) and at a molecular level by Fluorescence Correlation Spectroscopy (FCS). Moreover electrophysiological recordings on GUVs membrane patches allowed to characterize ion channel fluctuations, which were generated by PLN in these membranes. The data show that the PLN protein spontaneously inserts into lipid bilayers and that this generates distinct cation selective channel activity.

## Experimental

### Protein expression and purification

WtPLN was purified as described in Smeazzetto et al. 2013<sup>12</sup>. Briefly the protein was expressed in *E. coli* as a maltose binding protein (MBP) fusion protein. The lysate was passed through amylose resin (New England Biolabs, Ipswich, MA, USA) in

order to isolate the pure MBP-PLN fusion protein. The fusion protein was cleaved overnight at room temperature with a fully active TEV protease variant<sup>27</sup>. Subsequently PLN was purified by FPLC (Akta Purifier ÄKTAPrime™ plus, GE Healthcare Pittsburgh, PA, USA) using a reverse-phase column C18. Proteins were lyophilized, resuspended in 50 % Acetonitrile (Sigma Aldrich, Steinheim, Germany) and lyophilized again.

### Giant Unilamellar Vesicles Preparation

Giant Unilamellar Vesicles (GUVs) were prepared through electroformation, as previously described<sup>20,21</sup>. A lipid mixture of 3mg/ml diphytanoylphosphatidylcholine (DPhPC) (Avanti Polar, AL, USA) and 0.3 mg/ml Cholesterol (Sigma Aldrich, Steinheim, Germany) in chloroform was prepared. The fluorescent dye  $\beta$ -Bodipy ( $\beta$ -BODIPY® FL C5-HPC (2-(4,4-difluoro-5,7-dimethyl-4-bora-3a,4adiazas-indacene-3-pentanoyl) -1 hexadecanoyl-sn-glycero-3-phosphocholine, from Avanti Polar Lipids, AL, USA)) was added at 0.01% and 0.001% for imaging experiments and for FCS experiments, respectively. 10 $\mu$ l of the stock solution were deposited on each conductive side of two glass slides covered with ITO. The solvent was evaporated under vacuum for two hours to obtain a dry lipid film. The electroformation chamber was assembled joining the slides, separated by an O-ring. The chamber was filled with a Sucrose 500 mM aqueous solution; the electrical contact was provided by a copper tape connected to a pulse generator, set at a sinusoidal alternating voltage of 10 Hz frequency and 2 V pp amplitude for two hours.

### Lipids and PLN Labelling

Labelled  $\beta$ -Bodipy-GUVs were prepared as a mixture of DPhPC and Cholesterol (DPhPC-Chol 10/1 w/w) and a small quantity of fluorescently modified phospholipid ( $\beta$ -Bodipy, 0.01% w/w with respect to the total lipid amount). DPhPC was chosen because of its high stability at room temperature, which provides reliable and artifact-free electrical recordings of PLN activity. A small percentage of cholesterol, commonly present in cell membranes, was added to improve the similarity of the experimental model with biological membranes.<sup>28</sup> PLN was fluorescently labelled employing the commercial AnaTag 5-Tamra protein labeling kit from Anaspec (Fremont, CA). Briefly, 100  $\mu$ l of a 3mg/ml PLN stock solution (40% Ethanol in water) were mixed with 10  $\mu$ l of a conjugation buffer solution and, finally, to 8,8  $\mu$ l of the fluorescent tag solution. The reaction mixture was incubated for one hour at room temperature. The protein-Tamra conjugates were then purified through Amicon Ultra-0.5 mL centrifugal filters for protein purification with a 3 kDa cut off (Merck Millipore, Billerica, MA) according to the instruction of the manufacturer. The purified protein-Tamra conjugates were further incubated for one hour at room temperature with 10 mM DTT (dithiothreitol, from Sigma Aldrich, Steinheim, Germany) to avoid multiple binding of the fluorescent tag to phospholamban unit<sup>8</sup> and finally purified again in a Amicon column 3 kDa cut off. Tamra-PLN was stored at -20°C.

### Laser Scanning Confocal Microscopy (LSCM)

LSCM experiments were carried out with a laser scanning confocal microscope Leica TCS SP2 (Leica Microsystems GmbH, Wetzlar, Germany) equipped with a 63x water immersion objective; chromophores were excited by 488-nm and 561-nm laser lines. 60  $\mu\text{l}$  of GUVs dispersion in Sucrose 500 mM were put in a chamber (Lab-Tek® Chambered # 1.0 Borosilicate Coverglass System, Nalge Nunc International, Rochester, NY, USA) and then diluted by adding 180  $\mu\text{l}$  of a buffer solution containing KCl 250 mM and Hepes 5 mM pH 7.4. 4  $\mu\text{l}$  of the purified Tamra-PLN solution were added to the GUV dispersion. The sample was incubated for thirty minutes at room temperature before both LSCM acquisition and FCS measurements were performed.

### Fluorescence Correlation Spectroscopy (FCS)

The FCS measurements were carried out with a ISS module (ISS, Inc. 1602 Newton Drive Champaign, IL, USA) equipped with two APD (Avalanche Photodiodes) with 500-530 nm and 607-683 nm BP. FCS measurements were carried out by exciting the fluorescent probe (Alexa 568 or Tamra) at 561 nm and acquiring the fluorescence emission between 607 and 683 nm.

The autocorrelation function of the fluorescence intensity ( $G(\tau)$ ) is calculated as a function of the fluctuations of the signal from the averaged value,  $\delta(t) = I(t) - \langle I(t) \rangle$ , as:<sup>29,30</sup>

$$G(\tau) = \frac{\delta I(t)\delta I(t+\tau)}{\langle I(t) \rangle^2} \quad (1)$$

The models employed for the analysis of the autocorrelation functions (ACFs) take into account the shape and the exact size of the detection volume, which is approximated as 3D-ellipsoidal Gaussian shape with axial ( $z_0$ ) and lateral ( $w_0$ ) defining parameters, determined through calibration procedure carried out with reference fluorescent dye with known diffusion coefficient (we employed a 50 nM standard solution of Alexa 568,  $D = 332 \mu\text{m}^2\text{s}^{-1}$  in water at 25°C). For a three-dimensional Brownian diffusion mode in a 3D Gaussian volume shape, the ACFs profiles can be analyzed according to equation (2):

$$G(\tau) = \frac{1}{\langle c \rangle \pi^{3/2} w_0 z_0} \left( 1 + \frac{4D\tau}{w_0^2} \right)^{-1} \left( 1 + \frac{4D\tau}{z_0^2} \right)^{-1/2} \quad (2)$$

With  $\langle c \rangle$  the averaged fluorophore concentration (nM),  $D$  the diffusion coefficient of the probe ( $\mu\text{m}^2\text{s}^{-1}$ ). FCS curves were collected by exciting at 561 nm and acquiring the fluorescence emission between 607 and 683 nm (in order to collect the fluorescence emission due to Tamra-PLN). In order to take into account the residual presence of free Tamra after purification of the protein, the FCS curves were analyzed through multicomponent equation, combining the free 3D diffusion of Tamra in the aqueous region and a two component 2D

diffusion of phospholamban within the membrane (equation 3).

$$G(\tau) = \frac{1}{N} \left[ f_1 \left( 1 + \frac{4D_1\tau}{w_0^2} \right)^{-1} \left( 1 + \frac{4D_1\tau}{z_0^2} \right)^{-1/2} + f_2 \left( 1 + \frac{4D_2\tau}{w_0^2} \right)^{-1} \right] \quad (3)$$

### Viscosity measurements

The viscosity measurements were carried out with a Paar Physica UDS200 rheometer working at  $25 \pm 0.1$  °C (Peltier temperature control system).

### Estimation of Phospholamban reduced radius according to SD model

It has been demonstrated<sup>31</sup> that the Saffman-Delbruck (SD) approximation is a valid model to describe the diffusion of a membrane inclusion, when the size of the membrane inclusion (represented by its radius  $a$ ) is considerably lower than a characteristic lengthscale, the so-called hydrodynamic lengthscale ( $l_{SD}$ ), defined by the ratio of the membrane viscosity ( $\eta$ ) to the 3D bulk viscosity of the internal and surrounding media of the GUVs  $\mu_1$  and  $\mu_2$ . When the reduced radius of the inclusion,  $\epsilon$ , defined as  $\epsilon = a/l_{SD} = a(\mu_1 + \mu_2)/\eta$ , is  $\ll 1$ , the SD approximation is valid. The reduced radius  $\epsilon$  of the Phospholamban (monomer and pentamer) embedded in the membrane can be calculated assuming the radius  $a$  of the monomer ( $\approx 10$  Å) and of the pentamer ( $\approx 30$  Å); the measured internal and external bulk viscosity values are  $\mu_1 = 1.57 \pm 0.02$  mPa·s for the internal solution of the GUVs (0.5M sucrose) and  $\mu_2 = 1.09 \pm 0.01$  mPa·s for the external medium (Hepes 5 mM, KCl 250 mM). The surface viscosity of the DPhPC-Chol membrane is  $2.1 \cdot 10^{-9}$  Pa·s·m when we assume literature values for the fluid phase of DPhPC-DPPC lipid mixtures.<sup>31</sup> The estimated reduced radius values  $\epsilon$  are thus  $\epsilon \approx 1.3 \cdot 10^{-3}$  for the PLN monomer and  $\epsilon \approx 3.8 \cdot 10^{-3}$  for the pentamer. We are thus in the SD approximation.<sup>31,32</sup>

### Electrophysiology

The un-labelled wtPLN, previously solubilized in water, was added to the un-labelled GUVs solution at a final concentration of ca. 0.3  $\mu\text{M}$ . WtPLN was incubated at least 30 minutes with the GUVs solution to allow spontaneous reconstitution. The solution containing WtPLN and GUVs was then added to a recording chamber (Warner Instruments, Hamden, CT) filled with a buffer solution containing KCl 250 mM and HEPES 5 mM, pH 7.4 (with KOH). Most of the sucrose-containing GUVs were immobile on the bottom of the plastic dish and accessible for patch clamp recordings. The patch pipette was filled with the same buffer solution of the bath medium and recordings of channel currents on PLN reconstituted in GUVs were done in excised patches. In control experiments we also performed recordings on GUVs in the absence of PLN. None of these recordings revealed any channel like activity.

Patch-clamp pipettes were pulled from Sutter capillary glass (Sutter instrument company, CA) on a Flaming/Brown type puller (Sutter P-87, Sutter instrument company, CA) and fire



polished on a microforge (Narishige International U.S.A). Polished pipettes had resistances between 10 and 30 M $\Omega$ . Ionic currents were recorded with an Axon Multiclamp 700B amplifier (Molecular Devices, Inc., Sunnyvale, CA) connected to a Digidata 1440 data acquisition board (Molecular Devices, Inc., Sunnyvale, CA) and controlled via pCLAMP 10 software (Molecular Devices, Inc., Sunnyvale, CA). Currents were sampled with 5 kHz after low pass filtering with 1 kHz. Data analysis was performed with the Clampfit-Software 10 (Molecular Devices, CA, USA) and Origin8 (OriginLab, Northampton, MA). The apparent single channel current amplitudes ( $I_{app}$ ) were determined by visual inspection of the current traces using the Clampfit software. For experiments on ionic selectivity the bath solution was exchanged through a multi valve perfusion system (Warner Instruments, Hamden, CT) with CsCl 250 mM and HEPES 5 mM, pH 7.4. Permeability ratio have been calculated using the Goldman-Hodgking-Katz equation (equation 4)

$$E_{inv} = \frac{RT}{zV} \ln \left( \frac{P_K [K^+]_{pip}}{P_{Cs} [Cs^+]_{bath}} \right) \quad (4)$$

Where R is the ideal gas constant, T is temperature (in Kelvin), F is the Faraday's constant,  $[K^+]_{pip}$  is the potassium ionic concentration in the pipette solution and  $[Cs^+]_{bath}$  is the cesium ionic concentration in the bath solution. We considered the reverse potential obtained by experimental I/V curve (Figure 5B).

## Results and discussion

### Spontaneous PLN reconstitution in GUVs

The reconstitution of PLN into GUVs was monitored on a LSCM employing Tamra labelled red PLN (Tamra-PLN) and  $\beta$ -Bodipy labelled green GUV phospholipids ( $\beta$ -Bodipy-GUVs). Labelled  $\beta$ -Bodipy-GUVs were prepared as a mixture of DPhPC and Cholesterol. The use of a DPhPC bilayer also allows for a straightforward comparison of the present data with recent electrical recordings of PLN activity on BLMs.<sup>12,15</sup> Tamra-PLN was incubated for 30 minutes with  $\beta$ -Bodipy-GUVs to allow spontaneous reconstitution.

Figure 1 shows representative confocal images, which were recorded on the same GUV 30 min after incubation of Tamra-PLN with  $\beta$ -Bodipy-GUVs. The GUV bilayer is clearly identified in the green channel by the emission of  $\beta$ -Bodipy (Figure 1A) and the PLN protein by the red fluorescent emission of Tamra-PLN (Figure 1B). In this image a very low fluorescent background can be observed in the aqueous environment surrounding the GUVs bilayer. This background signal can be assigned to residual free dye, which is still present in the sample after the purification of Tamra-PLN conjugates (see also Figure S1-S2). Nevertheless, the distinct localization of Tamra emission in the GUV bilayer indicates that Tamra-PLN

reconstitutes into the lipid membrane. This is further underscored by the overlay of the green and the red channel images in Figure 1C. The perfect overlap of  $\beta$ -Bodipy and Tamra fluorescence emission (in yellow) highlights the colocalization of the protein in the GUV bilayer. The confocal images prove on a microscopic length-scale the spontaneous embedding of the protein into the GUV bilayer; this occurs upon simple incubation of PLN with the vesicles.

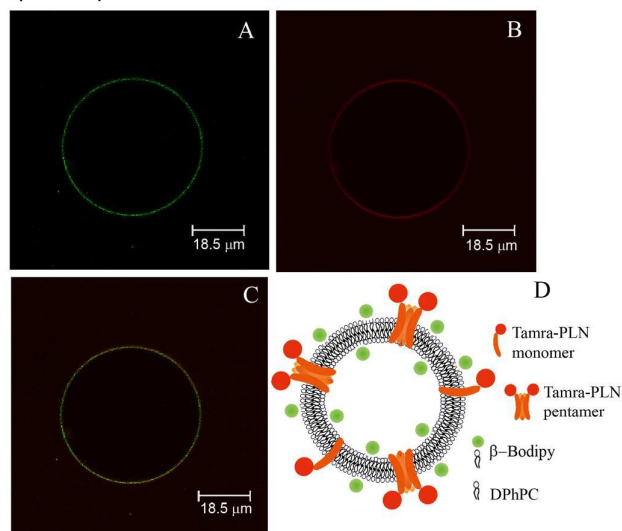


**Figure 1.** LSCM image of Tamra-PLN reconstituted in  $\beta$ -Bodipy GUVs: A) LSCM image acquired in the first photomultiplier (PMT)  $\beta$ -Bodipy-GUVs (green,  $\lambda_{excitation}$  488 nm,  $\lambda_{emission}$  498-530 nm); B) LSCM image acquired in the second PMT Tamra-PLN (red,  $\lambda_{excitation}$  561 nm,  $\lambda_{emission}$  600-700 nm); C) overlay of the first and second PMT LSCM images (the yellow regions highlight the overlapping of fluorescence emission of the two fluorescent probes,  $\beta$ -Bodipy and Tamra); D) Schematic representation of the reconstituted Tamra-PLN in  $\beta$ -Bodipy-GUVs.

Many elaborate reconstitution methods had to be developed in the past to incorporate transmembrane proteins into GUVs; these included detergents, fusion or dehydration of proteoliposomes and electroformation from native membranes.<sup>24,26,33</sup>

Here we show that PLN is able to embed into a membrane by spontaneous incorporation. In order to monitor the mobility of the protein within the bilayer at a molecular length scale, we investigated the diffusion of PLN inside the GUV membrane by FCS (Figure 2 and 3).

The hydrodynamic behavior of proteins in a lipid bilayer is described by the Saffman and Delbruck (SD) model and its more recent modifications, as the diffusion of a cylindrical inclusion of radius  $a$  embedded in a membrane of viscosity  $\eta$  (see the experimental section for details).<sup>31,32,34-36</sup> The SD model can predict the 2D diffusion coefficient expected both for the monomeric and the pentameric form of PLN, assuming that 10 Å and 30 Å are the diameter of the cylinders representing PLN in its monomeric and pentameric form,

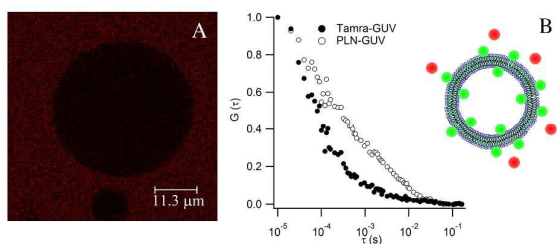


**Figure 2.** (A) Representative LSCM image acquired for Tamra incubated with  $\beta$ -Bodipy-GUVs ( $\lambda_{\text{excitation}}$  561 nm,  $\lambda_{\text{emission}}$  600-700 nm); (B) normalized FCS curves acquired for: the bare Tamra (filled circles) and PLN-Tamra (empty circles) incubated with  $\beta$ -Bodipy-GUVs.

respectively.<sup>11,37</sup> The expected values for the 2D translational diffusion coefficient in the membrane can be thus estimated as  $1.17 \mu\text{m}^2\text{s}^{-1}$  for the monomer and  $0.99 \mu\text{m}^2\text{s}^{-1}$  for the pentamer. These two values are very close, since the 2D diffusion coefficient of a membrane inclusion is mainly determined by the high viscosity of the lipid diffusing medium, and to a lesser extent by the size of the inclusion.<sup>31,32,38,39</sup> Therefore the two forms cannot be distinguished by the analysis of the experimental curves. The FCS data were analyzed with a two component diffusion model, considering the measured ACFs as a combination of the 3D diffusion of a residual percentage of free Tamra left after the purification procedure (whose diffusion coefficient in the experimental condition is equal to  $280 \mu\text{m}^2\text{s}^{-1}$ , see SI for details)<sup>40</sup> and the 2D diffusion of the Tamra-PLN in the membrane (equation 3). Keeping the diffusion coefficient of free Tamra and of Tamra-PLN fixed ( $280 \mu\text{m}^2\text{s}^{-1}$  for Tamra and  $1 \mu\text{m}^2\text{s}^{-1}$  for Tamra-PLN, which can be assumed as an approximated theoretical 2D diffusion coefficient value both for the monomer and the pentamer) it is possible to reproduce the experimental FCS curves, as clearly highlighted by the experimental and corresponding fitting curves reported in Figure 3B and by the related curve fit residuals (Figure 3C), while some variability in the profiles of the FCS curves is observed and can be fully attributed to a variable percentage of reconstituted protein in the membrane in different GUVs or different regions of detection and to possible effects on the fluorescence quantum yield of TAMRA probe due to protein aggregation. Thus, the LSCM images and the consistent fitting curves of FCS data confirm that Tamra-PLN spontaneously reconstitutes in the GUV membranes upon incubation with GUVs; the PLN protein accumulates in the membranes and freely diffuses within the GUV bilayer. The spontaneous incorporation of PLN into the bilayer is probably due to the small size of the PLN protein and the highly hydrophobic properties of the single span transmembrane helix.

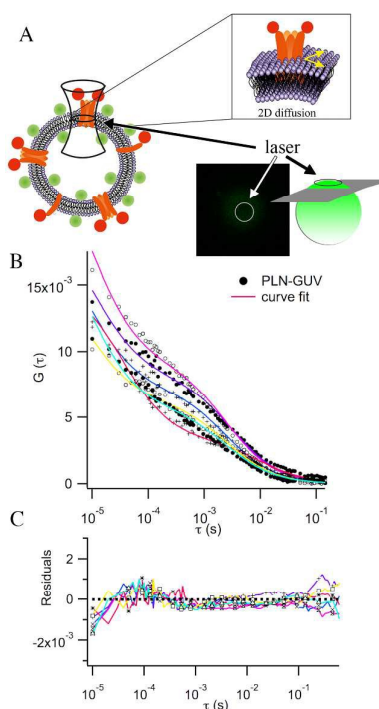


**Figure 3.** (A) Scheme of FCS measurement on top of the GUVs to monitor Tamra-PLN 2D diffusion within the membrane; (B) representative FCS experimental curves obtained for Tamra-PLN incubated with  $\beta$ -Bodipy-GUVs (circles) and curve fits (continuous red line) according to a 3D-2D two component diffusion (equation 3); (C) Curve fit residuals of the displayed experimental curves.

#### Functionality of PLN by electrophysiological recordings in membrane-patches on GUVs

The electrical activity of PLN reconstituted in GUVs was investigated in small membrane areas (Figure 4A) with the patch clamp technique on excised patch in the inside-out configuration. For electrical recordings the purified recombinant wtPLN (not labelled) was used in order to compare the present data with previous recordings of PLN generated channel activity in traditional BLMs.<sup>12</sup> After 30 minutes incubation of PLN with GUVs, single channel-like events were recorded as shown in Figure 4B.

Well-defined current fluctuations between a closed and open state were identified at both positive and negative potentials (Figure 4B), meaning that the channel has an Ohmic conductance. Moreover a further sub-conductance level was present and can occur concomitant and additive to the big conductance (Figure 5A). Due to the advantageous signal to noise ratio of single channel measurements in excised patches compared over BLM recordings, openings of the small conductance were well resolved at all the voltages. Figure 4C shows the linear  $I/V$  relation of large and small unitary currents. It is worth noting that the same Ohmic channel like activity of PLN with two conductance levels and long open and closed times was also found when PLN was reconstituted in planar lipid bilayers.<sup>15</sup> Most important is that the conductance

values and the gating properties in the two systems are the same. While we measure here 17.5 pS and 6.2 pS for the large and small conductance respectively (Figure 4) the corresponding values in BLM recordings were 18 pS and 8 pS.<sup>12,15</sup> With respect to gating of the PLN generated channel it is worth noting that the dwell times for the open and closed state are in the order of some 100 ms to seconds.<sup>12</sup>

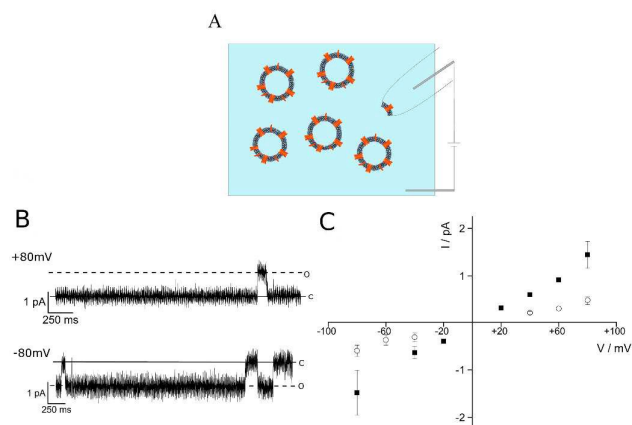


**Figure 4.** PLN reconstituted in GUVs generates single channel fluctuation. (A) Schematic representation of excised patch configuration of patch clamp measurements. (B) Example of unitary current traces recorded at +80 mV and -80 mV under symmetrical conditions with 250 mM KCl in 5 mM Hepes (pH 7.4), open (o, dashed line) and closed (c, continuous line) levels are highlighted in figure. (D) Current/voltage relation of small (empty circle) and big (filled square) conductance obtained under the same conditions as in experiment of Figure 4C. Data are mean  $\pm$  standard deviation of 4 independent experiments. Each data point for the small and large conductance is the mean value of at least 6 individual fluctuations.

Moreover Figure 6A shows examples of unitary current traces which were recorded at clamp voltages of -80, -60, +60, +80 mV under asymmetrical conditions with 250 mM KCl in the pipette and 250 mM  $\text{CaCl}_2$  in the bath. The resulting I/V curve shows that the current did not reverse in the window of test voltages (Fig. 6B). The absence of negative current shows that the protein conducts no positive charges from the bath medium, which is at ground, into the pipette; this means that the PLN channel is not conducting  $\text{Ca}^{2+}$ . The present data are in agreement with results obtained in BLM recordings and they show that the PLN generated channel has no appreciable permeability to  $\text{Ca}^{2+}$ . The unusually long life times and absence of  $\text{Ca}^{2+}$  permeability are found when PLN is reconstituted in BLMs and GUVs (e.g. Figure 4,5,6). This robust characteristic of PLN generated channel activity together with the apparent cation selectivity of the channel, which can be recorded in different experimental systems<sup>12,15</sup> and with different techniques<sup>15,16</sup> underscores that the electrical activity is neither an artefact of the biomimetic model nor due to contaminants in the protein preparation. Hence PLN can spontaneously enter into membranes where it is able to form a conducting channel with distinct properties. The ion channel properties of PLN registered in GUVs are consistent with the

view that not only PLN as a monomer, but the PLN forming channel can modulate SERCA in the SR of cardiac myocytes by corrupting the charge balance system of the SR.<sup>12,13</sup> In further experiments we studied the selectivity of the PLN channel for  $\text{Cs}^+$ . The experiments were performed by replacing 250 mM KCl in bath solution with 250 mM CsCl. Figure 5A shows unitary current traces that were recorded at various holding potentials in asymmetrical solutions. The resulting current–voltage relation for the large and small conductances are displayed in Figure 5B.

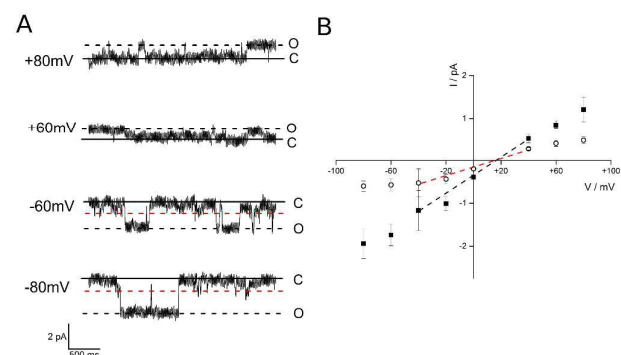


**Figure 5.** (A) Example of large conductance obtained under asymmetrical conditions with 250 mM KCl in 5 mM Hepes (pH 7.4) in the pipette and 250 mM CsCl in 5 mM Hepes (pH 7.4) in bath; open (o, dashed line) and closed (c, continuous line) and small conductance (red dotted line) levels recorded at -80, -60, +60 and +80 mV are highlighted in figure. (B) Current/voltage relation of large conductance (square) and small conductance (circle) obtained under the same conditions of experiments in Figure 5A. Mean  $\pm$  standard deviation of 7 recordings. The I/V relations of the small (red line) and the large conductance (black line) are quasi linear between +40mV and -40mV and reverse at +19mV. Each data point for the small and large conductance is the mean value of at least 6 individual fluctuations.

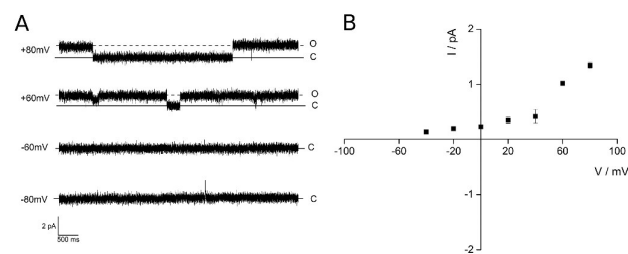


**Figure 6.** (A) Example of large PLN generated conductance obtained under asymmetrical conditions with 250 mM KCl in 5 mM Hepes (pH 7.4) in the pipette and 250 mM  $\text{CaCl}_2$  in 5 mM Hepes (pH 7.4) in bath; open (o, dashed line) and closed (c, continuous line) levels recorded at -80, -60, +60 and +80 mV are indicated. (B) Mean current/voltage relation  $\pm$  standard deviation of large conductance measured under the same conditions in 7 independent recordings.

It is important to note that the I/V curves reverse at a positive voltage e.g. at +19 mV. This means that the PLN generated channel is cation selective and prefers  $\text{Cs}^+$  over  $\text{K}^+$ . Using the Goldman–Hodgkin–Katz equation (equation 4) the reversal voltages give a permeability ratio  $P_{\text{K}}/P_{\text{Cs}}$  of ca. 0.5 meaning that the PLN channel conducts  $\text{Cs}^+$  about two times better than

$K^+$ . A higher permeability for the  $Cs^+$  ion, that has a bigger radius than  $K^+$ , (1.69Å and 1.33Å, respectively) suggests that the PLN forming channel is not a simple, non-specific hole. The pore forming amino acids must be able to dehydrate the  $Cs^+$  cation at lower energy than smaller cations.

## Conclusions

In the present work, we investigated PLN at a single molecule level by optical and electrophysiological techniques. First, we have characterized the spontaneous reconstitution of PLN in GUVs by optical techniques. LSCM and FCS experiments reveal that PLN embeds in the phospholipid bilayer and it moves in the membrane with a diffusion coefficient characteristic of membrane proteins. Moreover, the ion channel properties of PLN were analysed by electrophysiological experiments in excised patch of GUVs. Our results disclose that PLN generated channel activity is strictly correlated with a spontaneous insertion of the protein into the membrane and not an artefact of the lipid bilayer. The reconstituted PLN protein generates in GUVs a cation channel, characterized by two conductance levels; the same reversal potential registered for the two conductance levels suggests that both conductances are provided by the same pore. The channel exhibits a preference for  $Cs^+$  over  $K^+$  and does not conduct  $Ca^{2+}$ . A main finding of the present study is that the data on PLN generated channel fluctuations in GUVs are in good quantitative agreement with recordings of PLN activity in BLMs. The protein exhibits in both recording systems the same overall functional behaviour including two similar conductance states and characteristic long open and closed dwell times. Also the selectivity of the channel, which passes  $K^+$  but no  $Ca^{2+}$ , is the same in both recording systems. This means that solvents, which remain to some extent in the membrane of BLMs<sup>41</sup> but not in GUVs, have no impact on the PLN generated channel activity. This is an important finding since a modification of the bilayer thickness by solvents could well have an impact on the hydrophobic match between bilayer and transmembrane domains<sup>42</sup> and hence on the function of a membrane protein in particular if the protein is as small as PLN. PLN generated channel activity was previously also recorded by the tip-dip technique from purified cardiac phospholamban in bilayers from phosphatidylserine and phosphatidylethanolamine. Moreover this study reported small PLN generated unitary channel fluctuations with two different conductances.<sup>13</sup> Other than in the present study, Kovacs and coworkers<sup>13</sup> found however a  $Ca^{2+}$  permeability of the channel. The reason for the discrepancy in the data remains unsolved. It could be due to the difference in the source of the protein, which is in one case the native purified protein<sup>13</sup> and in our case a recombinant protein. A different explanation for the discrepancy of the data could also be related to the different lipids, which were used to form the bilayers. While Kovacs et al.<sup>13</sup> included the negatively charged phosphatidylserine we only used neutral phospholipids. Recently data on  $K^+$  channels have shown that in particular anionic phospholipids can have drastic effects on the functional properties of channel.<sup>43</sup> In order to evaluate the functional significance of PLN generated channel activity it will be important to examine the effect of the dominating lipids in the membrane of the SR on the small membrane protein.

The overall system-independent recordings of channel fluctuations in different studies underscore that the PLN protein generates ion channel activity. The robust channel functionality in different biomimetic models strongly suggests that PLN can, presumably as pentamer, modulate SERCA activity. Moreover, the higher permeability of the PLN channel for  $Cs^+$  compared to  $K^+$  suggests that the amino acidic sequence of the protein forms a distinct selective pore, which is able to determine the ion permeability of the PLN pentamer. The preference for the large  $Cs^+$  ion implies that the selectivity is dominated by the energy for ion dehydration. Hence the mechanism, which is underlying this cation selectivity, cannot be explained by a simple size exclusion of the channel pore. We rather predict a distinct cation specific interaction of the permeant ion with the pore forming structure of the protein.

## Acknowledgements

Financial support from Ente Cassa di Risparmio di Firenze and PON01\_00937 CUP B51H11000260005 is acknowledged. S.S. thanks POR CRO FSE 2007-2013 project for her fellowship. C.M. and D.B. acknowledge financial support from MIUR through the project PRIN 2010-2011 grant 2010BJ23MN and G.T. support from LOEWE initiative iNAPO. All the authors would like to thank Dr. Emiliano Carretti for viscosity measurements.

## References

- 1 E. G. Kranias and R. J. Hajjar, *Circ. Res.*, 2012, **110**, 1646–60.
- 2 D. H. MacLennan and E. G. Kranias, *Nat. Rev. Mol. Cell Biol.*, 2003, **4**, 566–577.
- 3 F. Tadini-Buoninsegni, G. Bartolommei, M. R. Moncelli, R. Guidelli and G. Inesi, *J. Biol. Chem.*, 2006, **281**, 37720–7.
- 4 G. Inesi and F. Tadini-Buoninsegni, *J. Cell Commun. Signal.*, 2014, **8**, 5–11.
- 5 A. G. Schmidt, I. Edes and E. G. Kranias, *Cardiovasc. Drugs Ther.*, 2001, **15**, 387–396.
- 6 R. L. Cornea, L. R. Jones, J. M. Autry and D. D. Thomas, *Biochemistry.*, 1997, **36**, 2960–2967.
- 7 L. G. Reddy, L. R. Jones and D. D. Thomas, *Biochemistry*, 1999, **38**, 3954–3962.
- 8 M. Li, L. G. Reddy, R. Bennett, N. D. Silva Jr, L. R. Jones and D. D. Thomas, *Biophys. J.*, 1999, **76**, 2587–2599.
- 9 S. L. Robia, N. C. Flohr and D. D. Thomas, *Biochemistry*, 2005, **44**, 4302–4311.
- 10 E. M. Kelly, Z. Hou, J. Bossuyt, D. M. Bers and S. L. Robia, *J. Biol. Chem.*, 2008, **283**, 12202–12211.
- 11 V. V. Vostrikov, K. R. Mote, R. Verardi and G. Veglia, *Structure*, 2013, **21**, 2119–2130.
- 12 S. Smeazzetto, A. Saponaro, H. S. Young, M. R. Moncelli and G. Thiel, *PLoS One*, 2013, **8**, e52744.
- 13 R. J. Kovacs, M. T. Nelson, H. K. B. Simmerman and L. R. Jones, *J. Biol. Chem.*, 1988, **263**, 18364–18368.
- 14 S. Smeazzetto, M. De Zotti and M. R. Moncelli, *Electrochem. Commun.*, 2011, **13**, 834–836.
- 15 S. Smeazzetto, I. Schröder, G. Thiel and M. R. Moncelli, *Phys. Chem. Chem. Phys.*, 2011, **13**, 12935–12939.
- 16 S. Smeazzetto, A. Sacconi, A. L. Schwan, G. Margheri and F. Tadini-Buoninsegni, *Langmuir*, 2014, **30**, 10384–10388.



- 17 P. G. Merzlyak, L. N. Yuldasheva, C. G. Rodrigues, C. M. Carneiro, O. V. Krasilnikov and S. M. Bezrukov, *Biophys. J.*, 1999, **77**, 3023–3033.
- 18 D. J. McGillivray, G. Valincius, F. Heinrich, J. W. F. Robertson, D. J. Vanderah, W. Febo-Ayala, I. Ignatjev, M. Lösche and J. J. Kasianowicz, *Biophys. J.*, 2009, **96**, 1547–1553.
- 19 J. W. F. Robertson, J. J. Kasianowicz and S. Banerjee, *Chem. Rev.*, 2012, **112**, 6227–6249.
- 20 C. Montis, P. Baglioni and D. Berti, *Soft Matter*, 2014, **10**, 39–43.
- 21 C. Montis, S. Sostegni, S. Milani, P. Baglioni and D. Berti, *Soft Matter*, 2014, **10**, 4287–97.
- 22 S. Nappini, T. Al Kayal, D. Berti, B. Norden and P. Baglioni, *J. Phys. Chem. Lett.*, 2011, **2**, 713–718.
- 23 Y. Sun, C.-C. Lee, T.-H. Chen and H. W. Huang, *Biophys. J.*, 2010, **99**, 544–52.
- 24 D. Shayaa, M. Kreirb, R. A. Robbinsc, S. Wonga, J. Hammona, A. Brüggemannb and D.L. Jr. Minor, *Proc. Natl. Acad. Sci. USA.*, 2011, **108**, 12313–12318.
- 25 S. Aimon, J. Manzi, D. Schmidt, J. A. Poveda Larrosa, P. Bassereau and G. E. Toombes, *PLoS One.*, 2011, **6**, e25529.
- 26 M. Dezi, A. Di Cicco, P. Bassereau and D. Lévy, *Proc. Natl. Acad. Sci. USA.*, 2013, **110**, 7276–7281.
- 27 L. D. Cabrita, D. Gilis, A. L. Robertson, Y. Dehouck, M. Rooman and S. P. Bottomley, *Protein Sci.*, 2007, **16**, 2360–2367.
- 28 G. van Meer, D. R. Voelker and G. W. Feigenson, *Nat. Rev. Mol. Cell Biol.*, 2008, **9**, 112–124.
- 29 J. Ries and P. Schwille, *Bioessays*, 2012, **34**, 361–368.
- 30 K. Koynov and H.-J. Butt, *Curr. Opin. Colloid Interface Sci.*, 2012, **17**, 377–387.
- 31 E. P. Petrov, R. Petrosyan and P. Schwille, *Soft Matter*, 2012, **8**, 3552–3555.
- 32 E. P. Petrov and P. Schwille, *Biophys. J.*, 2008, **94**, L41–43.
- 33 N. Kahya, *Biochim. Biophys. Acta.*, 2010, **1798**, 1392–1398.
- 34 P. G. Saffman and M. Delbrück, *Proc Natl Acad Sci U S A.*, 1975, **72**, 3111–3113.
- 35 P. G. Saffman, *J. Fluid Mech.*, 1976, **73**, 593–602.
- 36 B. D. Hughes, B. A. Pailthorpe and L. R. White, *J. Fluid Mech.*, 1981, **110**, 349–372.
- 37 K. Oxenoid and J. J. Chou, *Proc. Natl. Acad. Sci. U. S. A.*, 2005, **102**, 10870–5.
- 38 G. Guigas and M. Weiss, *Biophys. J.*, 2006, **91**, 2393–2398.
- 39 Y. a Domanov, S. Aimon, G. E. S. Toombes, M. Renner, F. Quemeneur, A. Triller, M. S. Turner and P. Bassereau, *Proc. Natl. Acad. Sci. U. S. A.*, 2011, **108**, 12605–12610.
- 40 C. Montis, C. Maiolo, I. Alessandri, P. Bergese and D. Berti, *Nanoscale*, 2014, **6**, 6452–6457.
- 41 A. J. Williams, in *Microelectrode techniques: the Plymouth Workshop handbook*, eds. D. Ogden and C. The Company of Biologists, 1994, pp. 79–99.
- 42 A. Holt and J. A. Killian, *Eur. Biophys. J.*, 2010, **39**, 609–621.
- 43 P. Marius, M. Zagoni, M. E. Sandison, J. M. East, H. Morgan and A. G. Lee, *Biophys. J.*, 2008, **94**, 1689–1698.